

1 Introgression dynamics of sex-linked chromosomal 2 inversions shape the Malawi cichlid adaptive radiation

3 Authors: L. M. Blumer^{1†}, V. Burskaia^{2†}, I. Artiushin^{2†}, J. Saha^{2†}, J. Camacho Garcia², F.
4 Campuzano Jiménez², A. Hooft van der Huysdynen², J. Elkin³, B. Fischer¹, N. Van Houtte², C.
5 Zhou^{1,4}, S. Gresham², M. Malinsky⁵, T. Linderoth⁶, W. Sawasawa², G. Vernaz^{1,10‡}, I. Bista^{7,8}, A.
6 Hickey³, M. Kucka^{9§}, S. Louzada^{10¶}, R. Zatha¹¹, F. Yang¹², B. Rusuwa¹¹, M. E. Santos³, Y. F.
7 Chan^{13,9}, D. A. Joyce¹⁴, A. Böhne¹⁵, E. A. Miska^{16,1}, M. Ngochera¹⁷, G. F. Turner¹⁸, R. Durbin^{1,4*},
8 H. Svardal^{2,19*}

9 ¹Department of Genetics, University of Cambridge, Cambridge, England, CB2 3EH, UK.

10 ²Evolutionary Ecology Group, Department of Biology, University of Antwerp, 2020 Antwerp, Belgium.

11 ³Department of Zoology, University of Cambridge, Cambridge, CB2 3EJ, UK.

12 ⁴Wellcome Sanger Institute, Tree of Life, Wellcome Genome Campus, Hinxton, CB10 1SA, UK.

13 ⁵Institute of Ecology and Evolution, Department of Biology, University of Bern, Baltzerstrasse 6, 3012 Bern, Switzerland.

15 ⁶W.K. Kellogg Biological Station, Michigan State University, Hickory Corners, MI 49060, USA.

16 ⁷Senckenberg Research Institute and Natural History Museum, 60325 Frankfurt am Main, Germany.

17 ⁸LOEWE Centre for Translational Biodiversity Genomics, 60325 Frankfurt am Main, Germany.

18 ⁹Friedrich Miescher Laboratory of the Max Planck Society, Max-Planck-Ring 9, 72076 Tübingen, Germany.

19 ¹⁰Wellcome Sanger Institute, Wellcome Genome Campus, Hinxton, Cambridge CB10 1SA, UK.

20 ¹¹School of Natural and Applied Sciences, University of Malawi, Zomba, Malawi.

21 ¹²School of Life Sciences and Medicine, Shandong University of Technology, Zibo, China.

22 ¹³Groningen Institute for Evolutionary Life Sciences (GELIFES), University of Groningen, Nijenborgh 4, 9747AG Groningen, The Netherlands.

24 ¹⁴Evolutionary and Ecological Genomics Group, School of Natural Sciences, University of Hull, Hull, UK.

25 ¹⁵Leibniz Institute for the Analysis of Biodiversity Change, Museum Koenig Bonn, Adenauerallee 127, 53115 Bonn, Germany.

27 ¹⁶Department of Biochemistry, University of Cambridge, Cambridge, England, CB2 3EH, UK.

28 ¹⁷Department of Fisheries Headquarters, P.O. Box 593, Lilongwe, Malawi.

29 ¹⁸School of Environmental and Natural Sciences, Bangor University, Bangor, Gwynedd, LL57 2TH, Wales, UK.

30 ¹⁹Naturalis Biodiversity Center, 2333 Leiden, The Netherlands.

31

32 [†]These authors contributed equally to this work

33 [‡]Present address: Zoological Institute, University of Basel, 4051 Basel, CH

34 [§]Present address: Department of Translational Genomics, University of Cologne, 50931 Cologne, Germany

36 [¶]Present addresses: Laboratory of Cytogenomics and Animal Genomics, Department of Genetics and Biotechnology, University of Trás-os-Montes and Alto Douro, Vila Real, Portugal; BioSystems and Integrative Sciences Institute, Faculty of Sciences, University of Lisbon, Lisbon, Portugal.

39 *Corresponding author. Email: hannes.svardal@uantwerpen.be, rd109@cam.ac.uk

40 Abstract

41 Chromosomal inversions contribute to adaptive speciation by linking co-adapted alleles.
42 Querying 1,375 genomes of the species-rich Malawi cichlid fish radiation, we discovered five
43 large inversions segregating in the benthic subradiation that each suppress recombination over
44 more than half a chromosome. Two inversions were transferred from deepwater pelagic
45 *Diplotaxodon* via admixture, while the others established early in the *deep benthic* clade.
46 Introgression of haplotypes from lineages inside and outside the Malawi radiation coincided with
47 bursts of species diversification. Inversions show evidence for transient sex linkage and a
48 striking excess of protein changing substitutions points towards selection on neuro-sensory,
49 physiological and reproductive genes. We conclude that repeated interplay between depth
50 adaptation and sex-specific selection on large inversions has been central to the evolution of this
51 iconic system.

52

53 Main

54 Understanding how biodiversity evolves is a fundamental question in biology. While some
55 evolutionary lineages remain virtually unchanged over hundreds of millions of years (1), others
56 give rise to a great diversity of species over short evolutionary timescales (2). Adaptive
57 radiations are particularly remarkable examples of explosive diversification, with many
58 ecologically, morphologically, and behaviourally differentiated species emerging rapidly from a
59 common ancestor. It is still not well understood how evolutionary lineages can produce such
60 bursts of organismal diversity, but recent insights from genome sequencing point to a widespread
61 contribution of “old” genetic variants (3), often introduced into populations by hybridisation (4),
62 and reused in new combinations that provide adaptation to novel ecological niches (5). A
63 conundrum, however, is the role of meiotic recombination in this process. On the one hand,
64 recombination can create beneficial combinations of adaptive alleles (6). On the other hand,
65 recombination can break adaptive combinations apart (7), especially in the face of gene flow,
66 producing unfit intermediates (8), and impeding speciation (9).

67 Chromosomal inversions – stretches of DNA that are flipped in their orientation – provide a
68 mechanism to break the apparent deadlock between the beneficial and detrimental effects of
69 recombination on species diversification, by strongly suppressing recombination between the
70 inverted haplotype and its ancestral configuration (7, 10, 11). Inverted haplotypes acting as
71 “supergenes” can link together adaptive alleles that confer a fitness advantage in a specific
72 environmental context or species background (12). In recent years, inversions have increasingly
73 been found to contribute to adaptation (13, 14), genetic incompatibilities (15), assortative mating
74 (16), sexual dimorphism (17, 18), mating systems (19), social organisation (20), life-history
75 strategies (21) and other complex phenotypes (11). Inversions are more common between
76 sympatric than allopatric sister species in fruit flies (22), rodents (23), and passerine birds (24),

77 pointing to their involvement in speciation with gene flow. However, despite their evolutionary
78 relevance in other systems, there is relatively little information on their role in shaping large
79 vertebrate adaptive radiations (25–28).

80 With over 800 known extant species, Lake Malawi cichlids constitute the most species-rich
81 recent vertebrate adaptive radiation (29, 30). The radiation was able to unfold and generate
82 extraordinary morphological and ecological diversity, despite repeated hybridisation (31, 32) and
83 conserved fertility across species (33). Intriguingly, previous studies found broad genetic
84 association peaks for a behavioural phenotype important in assortative mating (34) in genomic
85 regions that showed suppressed recombination in crosses of Malawi cichlid species (35). This
86 raises the question of whether recombination-suppressing mechanisms such as inversions
87 contributed to the adaptive diversification of Malawi cichlids.

88 Here we show that five large inversions segregate across and within many species and groups in
89 the Lake Malawi radiation, and systematically investigate their evolutionary histories and
90 functions. By suppressing recombination, large chromosomal inversions can cause affected
91 genomic regions to show evolutionary histories consistently distinct from the rest of the genome
92 (36, 37). To detect regional deviations from the genome wide evolutionary history we obtained
93 whole genome sequencing (WGS) data from 1,375 individuals of 240 Malawi cichlid species
94 (table S1), detected 84 million single nucleotide polymorphisms (SNPs), and first inferred
95 genome-wide relationship patterns as a backbone (Fig. 1, fig. S1) (see materials and methods).
96 Previous work suggested that the Malawi radiation evolved through serial diversification of three
97 subradiations from a riverine-like ancestor (31): 1. A pelagic grouping of the mostly mid-water
98 *Rhamphochromis* and mostly deep-living *Diplotaxodon*; 2. an ecologically and morphologically
99 highly diverse *benthic* subradiation consisting of three subgroups – *deep benthics*, *shallow*
100 *benthics*, and semi open-water *utaka*; and 3. the predominantly rock-dwelling *mbuna*. The
101 generalist-like stem lineage is represented today by the Malawi cichlid species *Astatotilapia*
102 *calliptera* (which provided the reference genome for the present study) (31, 38). Phylogenetic
103 inference on our larger dataset confirms these major groupings and supports the branching order
104 (Fig. 1).

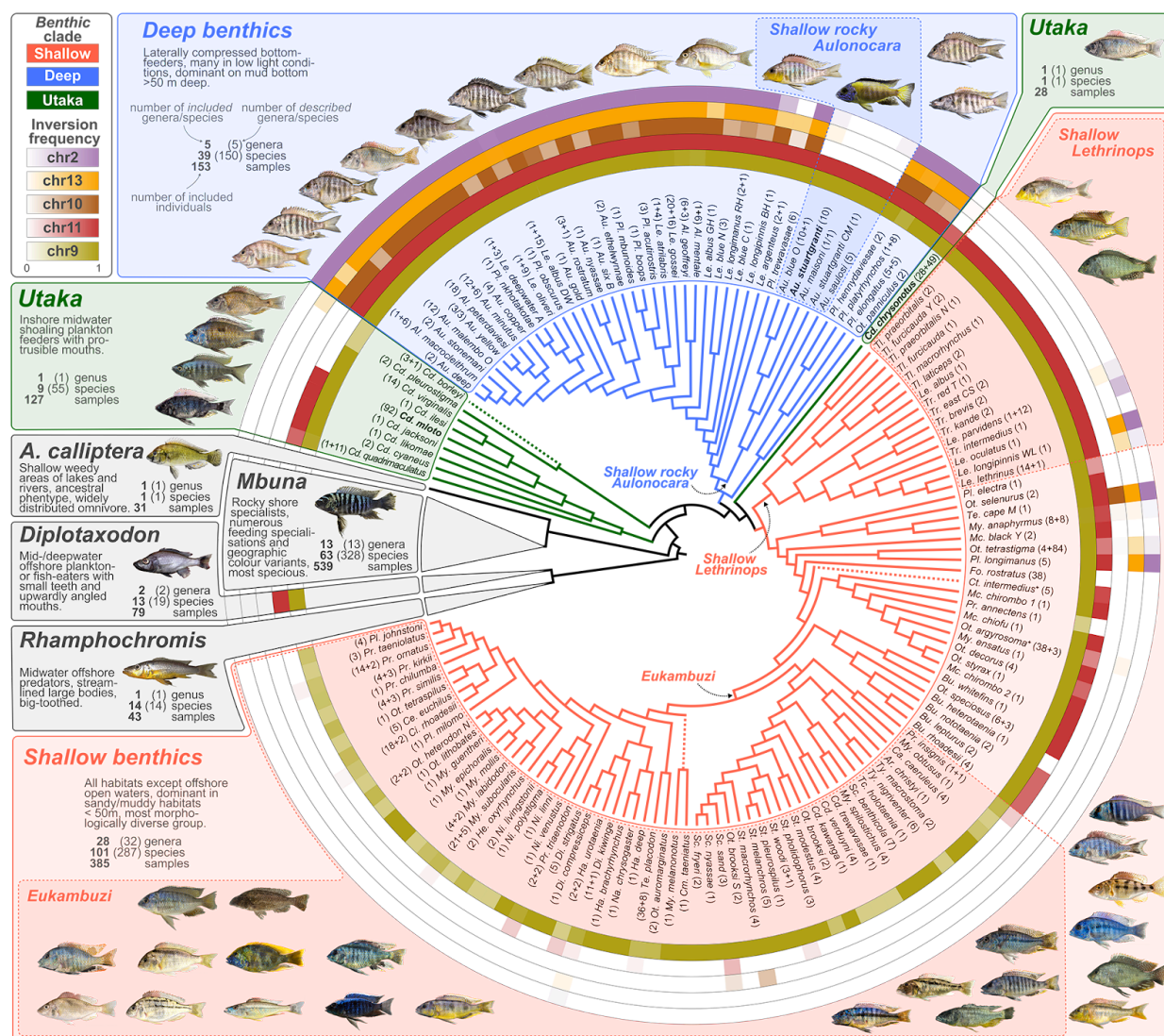
105 Large inversions suppress recombination

106 We identified extensive genomic outlier regions consistent with polymorphic inversions on five
107 chromosomes (2, 9, 10, 11 and 13), each spanning more than half a chromosome (between 17
108 and 23 Mbp), using a clustering approach on our SNP data set (Fig. 2A, top panel, figs. S2, S3)
109 (see materials and methods). A windowed principal component (PC) analysis (37, 39) of genetic
110 variation revealed that these regions showed relationships among species of the diverse *benthic*
111 clades of Malawi cichlids which were dramatically different from the rest of the genome
112 (Fig. 2A, bottom panel, fig. S4). While in the rest of the genome PC1 tended to separate the three
113 *benthic* subclades, in the focal regions three distinct clusters emerged that separated different

114 groups of individuals and explained a much higher proportion of the genetic variance (fig. S5).
115 Individuals in the intermediate cluster showed strongly increased heterozygosity as expected for
116 the heterozygous state of two divergent haplotypes (fig. S6). An exception to this was
117 chromosome 9, where only two clusters (one with increased heterozygosity) emerged, consistent
118 with the absence of one homozygous state. Overall, with double crossover events in only two
119 *deep benthic* individuals, the clustering was consistent with nearly complete recombination
120 suppression between inverted and non-inverted haplotypes (fig. S7) as observed in other systems
121 (22, 37, 40).

122 Using a combination of cytogenetics with long and linked read sequencing and *de novo*
123 chromosome-level assembly of all five major clades of Malawi cichlids allowed us to confirm
124 and characterise inversions in the regions on chromosomes 2, 9, 11 and 13 (but not chromosome
125 10 due to the lack of appropriate samples, see materials and methods) (Fig. 2B-C, table S4, fig.
126 S8 to S19) and revealed additional smaller inversions that went undetected in the SNP analysis,
127 including: (1) a small inversion nested inside the large inversion on chromosome 2, located next
128 to the centromere (text S1, fig. S15 and (2) two adjacent inversions on chromosome 20 (text S1,
129 fig. S16).

130 To confirm the suppression of recombination between inverted and non-inverted haplotypes, we
131 performed an interspecific cross between *A. calliptera* and *Au. stuartgranti* and whole genome
132 sequenced 290 individuals up to generation F3 (table S5). The absence of switching between the
133 inversion-state clusters on chromosomes 9 and 11 on genomic PC1 axis in F2 and F3 individuals
134 confirmed that recombination was fully suppressed in inversion regions of heterozygous F1s
135 (Fig. 2E). Segregation ratios in F2s were Mendelian, except for the chromosome 11 inversion
136 which had a moderate deficiency of homozygotes for the *A. calliptera* haplotype (genotype
137 proportions 20:66:43; χ^2 test on Mendelian ratios $p=0.016$).



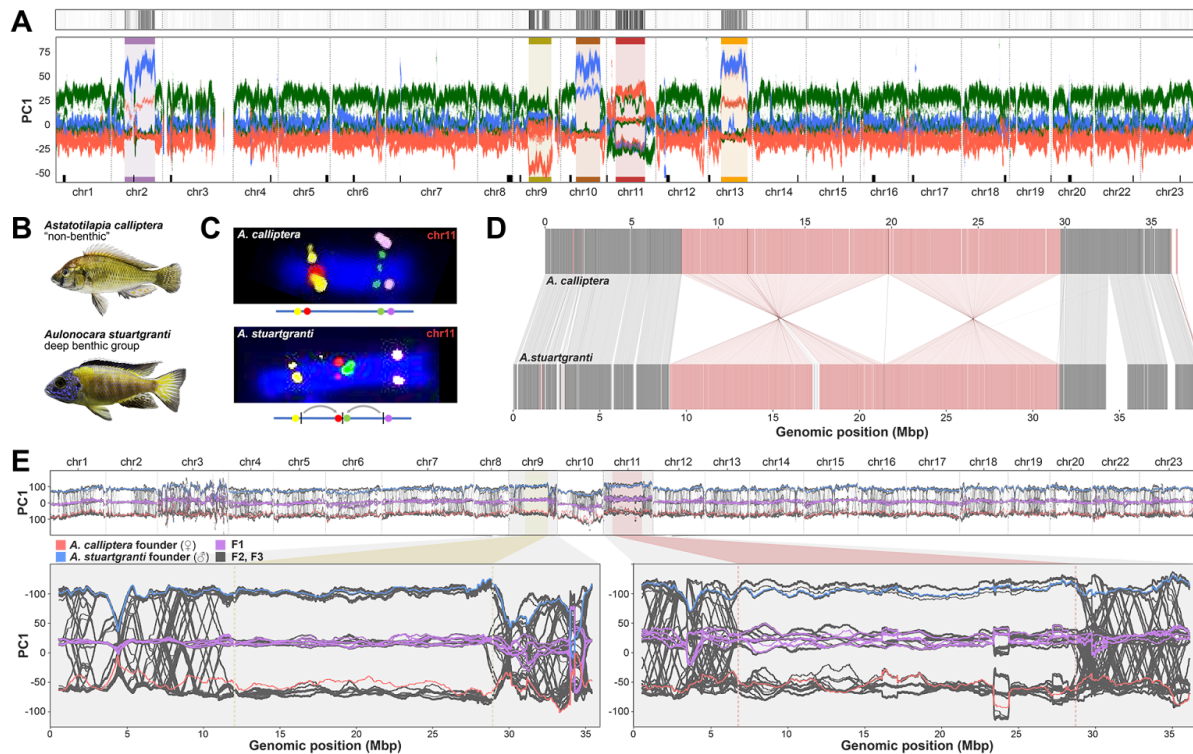
138

139 Fig. 1: Study system and prevalence of five large inversions. Consensus phylogeny of Malawi cichlid species
140 used in this study (data S1) with inversion frequency based on WGS and PCR-typing (see materials and methods)
141 shown in rings around the phylogeny (the same colours are used throughout the article). The *benthic* subradiation is
142 expanded to show the phylogenetic position of each species and to highlight subclades that we refer to in the main
143 text (*Shallow rocky Aulonocara*, *Shallow Lethrinops*, *Eukambuzi*). Note that *utaka* are not monophyletic in this
144 phylogeny. Non-*benthic* groups of Malawi cichlids (i.e., the *pelagic* subradiations of *Rhamphochromis* and
145 *Diplotaxodon*, the subradiation of predominantly rock-dwelling *mbuna*, and *Astatotilapia calliptera* – a species
146 distributed in rivers and margins around the lake that shares its putatively ancestral characteristics and genus
147 assignment with riverine haplochromines outside of the radiation) are each represented by a single grey triangle
148 approximately reflecting species richness relative to each other. Dashed lines indicate branches with unstable
149 placement. See data S1 and S2 for full phylogenies with branch lengths and support values. Annotations next to
150 species/clade names provide the numbers of sequenced/inversion-genotyped samples (additional samples which
151 were inversion-genotyped with PCR are indicated as + *n* in the annotation). Two taxa are annotated with “+” to denote
152 polyphyletic groups: *Otopharynx argyrosoma* contains a single *Cyrtocara moorii* individual and *Ctenopharynx*
153 *intermedius* contains two *Ctenopharynx pictus* individuals. Full species names are given in table S3 and inversion
154 frequencies by species in table S2. Species names for representative photographs are given in fig. S1. Tree files are
155 given in data S1 and S2. Species subject to further experimental investigation (see text) are highlighted in bold.

156 Inversions segregate within *benthic* subradiation

157 Next, we investigated the distribution of inversion states across the phylogeny based on a
158 multi-step PC approach to infer inversion genotypes for all 1,375 sequenced individuals
159 (“WGS-typing”) (Fig. 1, tables S7 and S8; fig. S20 and fig. S21), denoting as non-inverted or
160 *ancestral* the orientation of the outgroup species *Pundamilia nyererei* (fig. S22) and
161 *Oreochromis niloticus* (fig. S23). To further increase the number of genotyped individuals, we
162 identified TE insertions highly correlated with inversion state and PCR-typed these insertions in
163 an additional 401 individuals (see materials and methods, fig. S24, tables S9 to S11). Together,
164 these analyses revealed that all specimens of the *mbuna* and *Rhamphochromis* subradiations and
165 *A. calliptera* were fixed for the non-inverted, ancestral orientation for all five large inversions.
166 All *Diplotaxodon* specimens also lacked the inversions on chromosomes 2, 10 and 13 but
167 localized closer towards the cluster of inverted haplotypes than other non-*benthic* clades in the
168 PCA-based typing of the chromosome 9 and 11 inversions. In our *de novo* assembly for
169 *D. limnothrissa* both inversions are present (figs. S10, S25), suggesting that *Diplotaxodon* are
170 fixed for the inverted chromosome 9 and 11 haplotypes.

171 Among the *benthic* clades, the five inversions showed strikingly different frequencies across the
172 species: for chromosomes 2, 10, and 13, the inverted state was fixed or at high frequency in most
173 *deep benthic* species, but almost absent among *shallow benthic* species and *utaka*. For
174 chromosomes 9 and 11, the inverted states were fixed in most *benthics*, with the major exception
175 of a large monophyletic subclade of *shallow benthics* in which chromosome 11 was mostly fixed
176 for the ancestral non-inverted state and chromosome 9 mostly polymorphic. We will refer to this
177 group as “*eukambuzi*”, inspired by the local name “Kambuzi” for some members of this group
178 (Fig. 1). In summary, the distribution of inversion frequencies is consistent with a scenario in
179 which inversions on chromosomes 2, 10, and 13 rose to high frequencies in an ancestor of the
180 *deep benthic* lineage, while the inversions on chromosomes 9 and 11 rose to high frequency in
181 the ancestors of two non-sister groups – pelagic *Diplotaxodon* and *benthics* – but with one
182 monophyletic subgroup of the *benthics* (*eukambuzi*) retaining or re-gaining the non-inverted
183 ancestral state.



184

185 **Fig. 2: Characterisation of inversions.** (A) (Top panel): Identification of genomic regions from clusters of aberrant
186 phylogenetic patterns (see materials and methods). (Bottom panel): First genetic principal component in overlapping
187 1 Mbp windows along chromosomes, using the same colours for the *benthic* subclades as in Fig. 1. Outlier regions
188 from the top panel are highlighted and colour-labelled. Centromeric satellite regions (for inference see materials and
189 methods, text S1, fig. S17, table S6) are indicated as black rectangles on top of the X axis. (B) Representative
190 photographs of the species used in panels C-D: *Astatotilapia calliptera*, a lineage of the Malawi radiation distinct from
191 *benthics* from which the reference genome was produced, and *Aulonocara stuartgranti*, a species that genetically
192 belongs to the *deep benthic* group, but lives in shallow rocky habitats (clade *Shallow rocky Aulonocara* in Fig. 1).
193 According to WGS-typing, the species are expected to show opposite orientations for the chromosome 9 and 11
194 inversions. (C) Fluorescence in situ hybridisation (FISH) of markers on chromosome 11 left and right of the putative
195 inversion breakpoints show the expected non-inverted orientation (upper panel) in *A. calliptera*. In *Au. stuartgranti* we
196 see a double inversion (lower panel; see fig. S8 for FISH of chromosome 9). (D) Whole genome alignment of an ONT
197 duplex long-read assembly of *Au. stuartgranti* to the *A. calliptera* reference assembly (which was re-scaffolded with
198 chromosome conformation capture (Hi-C) data, see materials and methods) confirms the double inversion on
199 chromosome 11 (for other chromosomes see fig. S9). (E) Top: Windowed PC1 values of whole genome sequenced
200 founders and progeny of an interspecific cross. Among 290 F2 and F3 individuals no crossing-over events were
201 observed in the inversion regions of chromosomes 9 (bottom left) and chromosome 11 (bottom right), while
202 recombination was frequent in the flanking regions and on other chromosomes.

203 Origins and introgression patterns of the inversions

204 To better understand the evolutionary histories in inversion regions, we estimated genetic
205 divergence times between Malawi cichlid species for the five inversion regions (both the inverted
206 and non-inverted haplotypes) as well as for the remaining non-inverted regions of the genome
207 (Fig. 3A, fig. S26). Surprisingly, we found that, outside the inversions, *benthics* were least
208 divergent from *Diplotaxodon* and *A. calliptera* (top row in Fig. 3A), a pattern that is inconsistent
209 with the inferred phylogenetic position of *benthics* as a sister group to *mbuna* and *A. calliptera*
210 (e.g. ref. (31), Fig. 1, data S2), but rather suggests that *benthics* arose through admixture between
211 the *Diplotaxodon* and *A. calliptera* lineages after their respective splits from *Rhamphochromis*
212 and *mbuna* (Fig. 3B, see text S2 for more detailed discussion). Such a hybrid benthic origin
213 model also provides a parsimonious explanation for the sharing of the chromosome 9, 11 and 20
214 inversions between all *Diplotaxodon* and most *benthics* (figs. S9 to S12) (as indicated by Ⓐ in
215 Fig. 3B) and explains the general strong affinity of all inverted haplotypes to *Diplotaxodon*
216 (Fig. 3A, right panels).

217 The origins of non-inverted *benthic* haplotypes appear to be more diverse. The non-inverted
218 *benthic* chromosome 11 haplotype is closest to *A. calliptera* (Fig. 3A, row 3), as expected if this
219 haplotype was contributed from *A. calliptera* in the original founding of *benthics*. However,
220 previously inferred signals of gene flow between *shallow benthics* and *A. calliptera* relative to
221 *deep benthics* (31) and the relatively low heterozygosity of this haplotype (fig. S27), which is
222 mostly present among *eukambuzi*, could alternatively point to its later introgression from
223 *A. calliptera* (event Ⓒ in Fig. 3B).

224 For chromosome 9, *benthics* are almost fixed for the inversion with only some individuals,
225 mainly *eukambuzi*, being heterozygous. However, it is striking that the non-inverted haplotype
226 found in *benthics* is much more divergent from the rest of the Malawi radiation than any other
227 inversion haplotype and the rest of the *benthic* genome (Fig. 3A, row 2). To follow this up, we
228 produced a second SNP callset including a wide variety of related African cichlid species
229 (“haplochromines”) and computed ABBA-BABA tests (32, 41) (text S2, fig. S28, tables S12 and
230 S13, materials and methods). This revealed strong excess allele sharing of the non-inverted
231 *benthic* chromosome 9 haplotype with *Pseudocrenilabrus philander*, one of the few outgroup
232 species present today in the catchment of Lake Malawi ($D = 0.45$, block-jackknifing z-score 6.5;
233 FWER corrected $p = 4 \times 10^{-9}$). We conclude from this that the chromosome 9 non-inverted *benthic*
234 haplotype is not closely related to other Malawi haplotypes, but instead arrived in an ancestor of
235 *eukambuzi* through admixture with a lineage containing *Pseudocrenilabrus*-like genetic material
236 (Ⓑ in Fig. 3B).

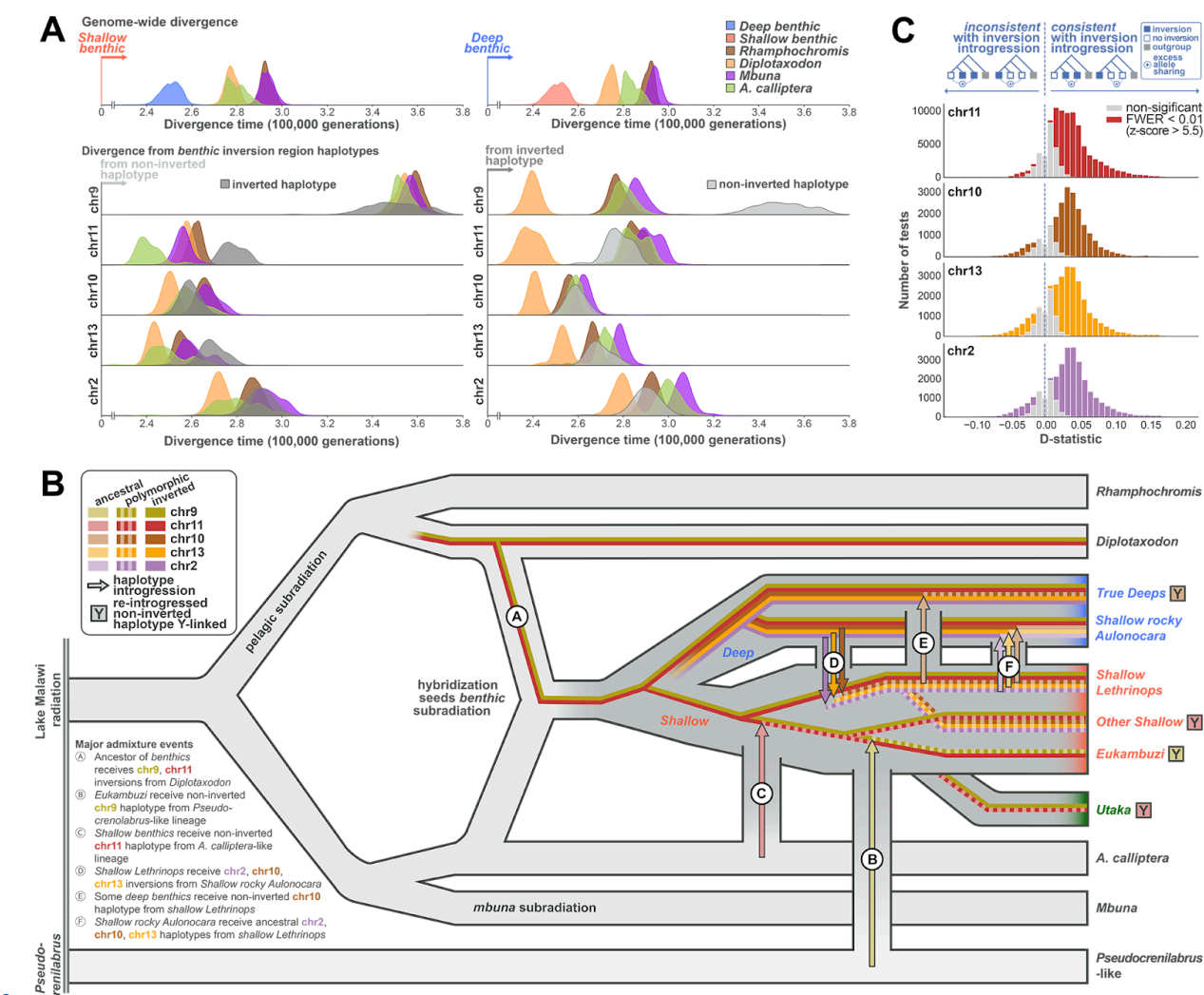
237 The remaining inversions on chromosomes 2, 10 and 13 are all common among *deep benthics*,
238 and rare or absent among *shallow benthics* and *utaka*, suggesting that they rose to high frequency
239 early in the *deep benthic* lineage (Fig. 3B). This is also consistent with the phylogenetic

240 relationships within the inversion regions (figs. S29 to S33), which suggest that the few cases of
241 *deep benthics* with non-inverted states and *shallow benthics* with inverted states are due to a
242 limited number of later gene flow events, the most consequential of which are indicated in
243 Fig. 3B (events D-F) (see text S2 and fig. S34 for a more comprehensive analysis). Most of
244 these events transmitted more than one inversion haplotype and also genetic material outside the
245 inversion regions (Fig. 3C) (41).

246 While there is evidence for each of the admixture and introgression events described in Fig. 3B
247 and fig. S34, other more complex scenarios are also possible. Furthermore, additional minor
248 introgression events and/or incomplete lineage sorting (ILS) are required to explain the final
249 patterns of occurrence of the inversions. However, the alternative hypothesis of random
250 segregation through incomplete lineage sorting giving rise to the observed patterns is not
251 supported. First, inference based on coalescent calculations yields a probability of only 0.02%
252 for retaining shared polymorphism among deep and shallow benthics at three inversions through
253 ILS (materials and methods) (28). Second, an ABBA-BABA analysis confirmed that signatures
254 of introgression outside of inversions were much more common when *deep benthic* and *shallow*
255 *benthic* species shared their inversion state, compared to cases where they differed in inversion
256 state (Fig. 3C), a pattern that is not expected under ILS.

257 Inversion divergence between deep and shallow-living lineages

258 All five inverted states are found at higher frequencies in deepwater-living species (fig. S35,
259 table S14). The corresponding regions show increased relative divergence and reduced
260 cross-coalescence rates (a measure of genetic exchange) compared to the rest of the genome,
261 and, for chromosomes 2, 10 and 13, also disproportionately high effect sizes in a
262 population-structure-corrected genome-wide association study between *deep* and *shallow*
263 *benthics* (materials and methods, Fig. 3A, figs. S36 to S40). Further, the inversion transmission
264 events inferred above (Fig. 3B, fig. S34) were often such that species living at depth atypical for
265 their clade (e.g., shallow-living rocky *Aulonocara* of the *deep benthic* clade and deep-living
266 *shallow benthic* species like *Trematocranus* sp. ‘Cape Maclear’) had received the inversion
267 haplotypes of species living at similar depths (fig. S35). Together, these observations support the
268 hypothesis that inversion haplotypes contributed to divergence along a depth gradient.



270 **Fig. 3: Evolutionary history scenario of inversion haplotypes.** (A) Density plots of pairwise sequence divergence 271 translated into divergence (coalescence) times assuming a mutation rate of 3×10^{-9} bp per generation (31). The top 272 panels show results for the genome outside the five large inversions, comparing all major clades against *shallow* 273 *benthics* (left) and *deep benthics* (right). Panels below the top row show divergence in inversion regions for the 274 non-inverted (left) and inverted (right) *benthic* haplotypes. (B) A simplified model for the evolutionary history of the 275 Malawi cichlid radiation, which includes several inversion haplotype transmission events. Vertical grey connections 276 indicate major gene flow events. Letter-labelled arrows indicate transfer of inversion-region haplotypes. For further 277 events see fig. S34. Lineages in which re-introgressed inversion region haplotypes of ancestral orientation apparently 278 play a Y-like role in sex determination (see Fig. 5 and main text) are indicated by Y . (C) Evidence for transfer of 279 inversion haplotypes through introgressive hybridisation. Histograms of ABBA-BABA statistics $D(P1, P2, P3,$ 280 *Outgroup*) calculated outside the inversions. For the different panels, we selected those ABBA-BABA tests for which 281 the inverted state of the respective chromosome is present in one of the two more closely related species P1 and P2 282 but absent in the other and ordered them such that P2 shared the inversion state (presence/absence) with P3. In 283 such a configuration, significantly positive values are suggestive of gene flow outside of inversions between the 284 species sharing inversion states, while significantly negative values suggest gene flow between species not sharing 285 inversion states. Under the null hypothesis of no inversion introgression, the statistic would be symmetric around 286 zero.

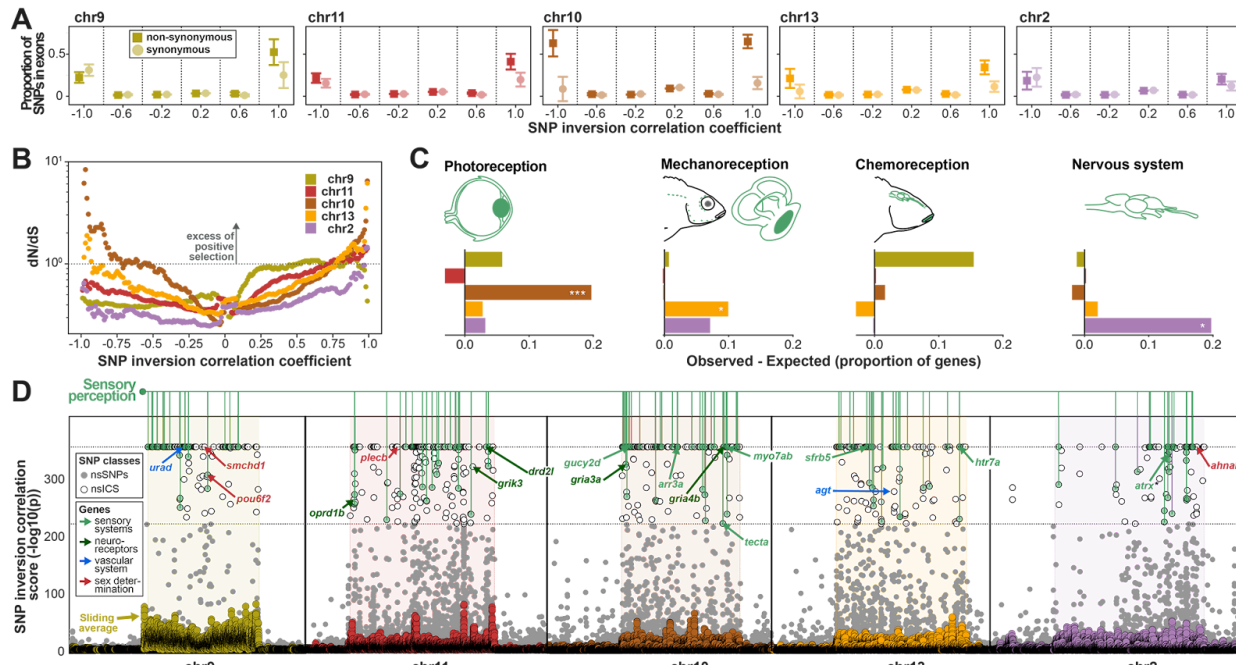
287 Pervasive signatures of adaptation on inversion haplotypes

288 Next, we investigated whether the evolution of inversion haplotypes was driven by adaptive
289 processes and could potentially constitute “supergenes” of co-adapted alleles. To identify genetic
290 variants relevant for the early evolution of inversion haplotypes, we computed correlation
291 coefficients and significance scores ($-\log_{10}$ p-value) between SNP and inversion genotypes (figs.
292 S41 and S42), where positive correlation coefficients correspond to derived SNP alleles on
293 inverted haplotypes and negative coefficients to derived SNP alleles on non-inverted haplotypes.
294 We expected the most highly inversion correlated SNPs (“ICS”) to contain variants relevant in
295 early inversion evolution.

296 ICS were much more likely to be located in protein coding regions compared to other (non-ICS)
297 SNPs on all five chromosomes (Fig. 4A) and showed a strong excess of non-synonymous
298 divergence in McDonald–Kreitman type tests (fig. S43), indicating that positive and/or relaxed
299 purifying selection contributed to inversion haplotype divergence. To confirm that there was a
300 component of positive selection, and not just drift due to relaxed purifying selection as expected
301 when a single haplotype rapidly raises in frequency (42), we calculated the normalised ratio of
302 non-synonymous to synonymous mutations (dN/dS). While dN/dS ratios can approach 1.0 when
303 selection is ineffective (complete relaxation of selection), values larger than 1.0 are only
304 consistent with adaptive evolution (text S2) (43). We found that dN/dS ratios increased with
305 increasing inversion correlation, with highly positive ICS showing $dN/dS \geq 1$ for all five
306 chromosomes (Fig. 4B, table S15). We confirmed with evolutionary simulations that such a
307 pattern is only expected in the presence of substantial numbers of positively selected variants
308 (text S2, figs. S44 and S45). Therefore, we conclude that widespread adaptive evolution
309 contributed to diversification between ancestral and inverted haplotypes on all five
310 chromosomes.

311 Interestingly, despite their general high differentiation, for many ICS both alleles were present in
312 at least one copy on both inverted and non-inverted haplotypes (37-72% of ICS, table S16). As
313 expected, this pattern of shared polymorphism across inversion orientations is even more
314 apparent for other (non-ICS) common variants (table S16) and suggests that despite their excess
315 divergence, recombination between inversion region haplotypes is not uncommon at
316 evolutionary timescales, potentially providing a mechanism to concentrate adaptive alleles on
317 such haplotypes.

318



319

320 **Fig. 4: Adaptive evolution of inversion haplotypes.** (A) Proportion of exonic SNPs, grouped by inversion 321 correlation coefficient intervals, relative to all SNPs within the same interval. A positive correlation coefficient 322 corresponds to the derived SNP allele being more common on the inverted haplotype, while a negative coefficient 323 corresponds to the derived SNP allele being more common on the non-inverted haplotype (ancestral orientation). (B) 324 dN/dS measured for SNPs as a function of inversion genotype correlation (see materials and methods). (C) Excess of 325 genes containing non-synonymous highly inversion correlated SNPs (nsICs) among all genes highly expressed in the 326 main sensory (green) and nervous system (blue). Expression data is based on the single-cell expression atlas of 327 developing zebrafish Daniocell (44). The tissues were grouped into the functional categories: vision (eye), 328 mechanoreception (lateral line, ear), chemoreception (taste, olfaction), and nervous system (neural). (D) 329 Non-synonymous SNPs (grey dots; if ICS: empty dots) and averaged ICS scores in 100 SNP rolling windows 330 (markers colour-coded according to inversion) on the five inversion chromosomes. We annotated nsICs located in 331 genes with high expression in zebrafish tissue groups related to sensory perception (same as in (C)). nsICs in 332 candidate genes discussed in the main text are annotated with arrows (if several were located in the same gene, the 333 highest nsICs is annotated) and color-coded by functional category (table S24).

334 Inversions contribute to sensory and physiological adaptation

335 To study functional roles of genes involved in inversion adaptations, we first analyzed expression
336 of the 315 genes from inversion regions with non-synonymous ICS (nsICS) in a multi-tissue
337 single-cell gene expression atlas of the zebrafish model (Daniocell database (44), text S3). We
338 found that individual inversions showed elevated expression in tissues related to vision,
339 mechanoreception, and the nervous system (FDR-corrected $p = 2 \times 10^{-4}$, 0.02, 0.04, respectively)
340 (Fig 4C, figs. S46 and S47, tables S17 to S20). As most of the associations were related to neural
341 and sensory tissues, we checked for overrepresentation of all neural and sensory tissues across all
342 five inversions, and found them to be significant (FDR-corrected $p = 6 \times 10^{-4}$, fig. S48, tables S21
343 and S22). We additionally tested for gene ontology (GO) enrichment of genes near ICS (see
344 materials and methods) and found sensory system-related categories in all five inversions
345 (table S23). Finally, we found vascular system-related categories functionally linked to responses
346 to hypoxia stress to be enriched in three inversions. All these findings are consistent with
347 adaptations related to changes in light, oxygen, and hydrostatic pressure along a depth gradient,
348 as observed in many aquatic organisms (45–47) including cichlids (31, 48, 49).

349 Among the 83 genes with two or more nsICS were strong candidate genes for depth adaptation
350 (tables S24 and S25), including genes involved in signal transduction in photoreceptor cells
351 (*arr3a*, *gucy2d*, *pou6f2*), otolith tethering (*tecta*), sound perception (*myo7ab*), kidney function
352 and blood pressure regulation (*urad*) and a master regulator of vasoconstriction (*agt*) (Fig. 4D,
353 text S4, table S24). Interestingly, some genes showed a close similarity between the amino acid
354 sequence coded by the inverted haplotype and that of *Diploptaxodon*, even when the relevant
355 inversion was not present in *Diploptaxodon* (e.g., *arr3a* on chromosome 10, see also Malinsky et
356 al. (31)) (fig. S49), which is consistent with a hybrid ancestry of *benthics* and subsequent
357 differential selection between recombination-suppressed inversion haplotypes. Intriguingly,
358 several genes harbour both positive and negative ICS, as expected under diversifying selection.

359 Consistent with their enrichment among sensory and neural tissues, we also found nsICS to be
360 significantly overrepresented among neuroreceptor genes that have been previously associated
361 with social (glutamate) and affiliative (oxytocin and arginine vasopressin/vasotocin, opioid
362 receptors, dopamine, serotonin) behaviour (50) (6 out of the 46 candidate genes, Fisher's exact
363 test $p=0.0011$) (table S26). These are three glutamate receptors (*gria3a* and *gria4b* on
364 chromosome 10, *grik3*, on chromosome 11), one opioid receptor (*oprd1b* on chromosome 11),
365 one dopamine receptor (*drd2l* on chromosome 11), and one serotonin receptor (*htr7a* on
366 chromosome 13) (fig. S49).

367 It is notable that the identified neurotransmitters are not only associated with fish social
368 behaviour in general, but have been specifically associated with bower building behaviour in
369 Malawi cichlids (51), a behavioural phenotype important for assortative mating (52), which has
370 previously been linked to the existence of supergenes (50) and associated with genetic

371 divergence peaks inside our chromosome 2 and 11 inversion regions (34). Following this up, we
372 found no significant correlation between bower type and the presence of the five inversions when
373 accounting for phylogeny (materials and methods; fig. S50, table S27; but see text S1),
374 suggesting that previously detected associations might be due to phylogenetic confounding.

375 Overall, our selection analyses suggest that widespread functional divergence in genes related to
376 sensory, vascular, and nervous systems occurred during the early evolution of inversion
377 haplotypes.

378

379 Inversions contribute to sex determination

380 Considering segregation patterns of inversion genotypes within species, we observed a notable
381 excess of inversion heterozygotes for chromosomes 9, 10, and 11 (deviation from within-species
382 Hardy-Weinberg-equilibrium, HWE, $p < 10^{-4}$, 0.0048, and 0.0133, respectively). This pattern
383 was most extreme for chromosome 9, for which despite the presence of 77 heterozygous
384 individuals across twelve species, not a single homozygous ancestral (non-inverted) state was
385 present in any *benthic*.

386 Since inversions are a common feature in the evolution of suppressed recombination on sex
387 chromosomes (53, 54), we hypothesized that the observed excess of heterozygotes could be due
388 to sex-linked inheritance (fig. S51). In the two species for which we had
389 gonad-examination-based sex assignment, we found a perfect correlation of sex with
390 chromosome 11 inversion state in *Copadichromis chrysonotus* (Fig. 5A, B; $n=28$, Fisher's exact
391 test p -value = 4.7×10^{-8}), while the other species, *Copadichromis mlobo*, was not variable for any
392 inversion. We further confirmed a significant chromosome 11 inversion–sex association among
393 107 laboratory-bred individuals from 11 broods of three species (Fig. 5C-E). Notably, in a
394 second laboratory population of one of these species (*O. tetrastigma*) with different geographic
395 origin, the chromosome 11 inversion was fixed for the inverted state, but there was a correlation
396 of sex with the chromosome 9 inversion state (Fig. 5E). This is consistent with previous
397 observations of multiple sex determination systems acting even within single Malawi cichlid
398 species (55, 56). In each case where there was an association, males tended to be heterozygous
399 and females homozygous for the respective inverted state as expected for XY-like sex
400 determination systems.

401 To further examine the extent of sex-linkage of inversions, we pooled data for each inversion
402 across species with at least one heterozygous sample (table S28). This revealed that, while
403 females tended to be homozygous for the inverted state, there was a significant association of
404 male sex with the heterozygous state for chromosomes 9, 10, and 11 (Fisher's exact test p -value
405 = 3.7×10^{-11} , 0.014, and 5.3×10^{-11} , respectively) (Fig. 5F, table S28) consistent with a widespread
406 role of the inversions in sex determination. That said, many species were not polymorphic for

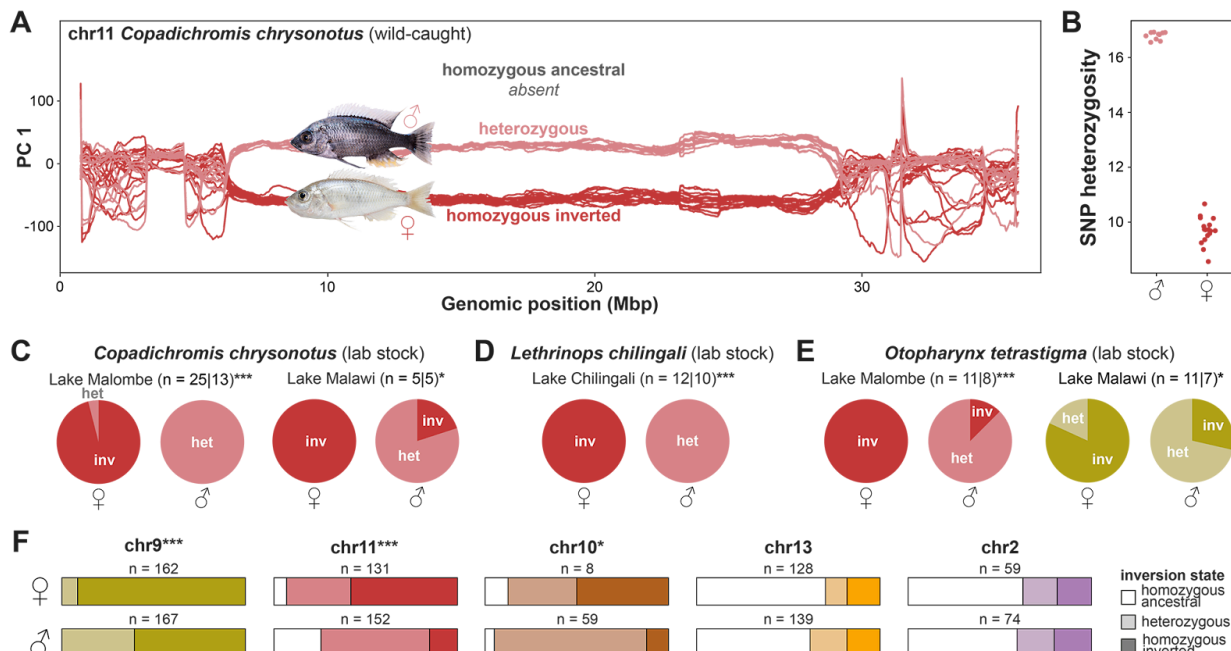
407 inversions and even within polymorphic species associations were usually not perfect (data S3)
408 suggesting additional genetic or environmental effects contributing to sex determination and a
409 rapid turnover of sex-linked function.

410 Given that the evolution of sex-determining regions often involves changes in gene expression
411 between male and female haplotypes, we obtained transcriptomic data of five tissues (muscle,
412 liver, brain, gills, gonads) for 11 males of *C. chrysonotus*, the species in which males were
413 heterozygous for the chromosome 11 inversion while females were fixed for the inverted state,
414 and investigated allele specific expression (ASE). Among genes with significant ASE (fig. S52,
415 text S3) there was a moderate bias towards lower expression of the Y-like non-inverted
416 haplotype, a pattern seen in many organisms (57). Further, lacking access to appropriate female
417 samples, we obtained equivalent data for eleven male *C. molo*, the congeneric species fixed for
418 the derived chromosome 11 inversion state, to perform differential gene expression (DE) analysis
419 between the two inversion states (fig. S53). Several of the significant ASE and DE genes (FDR <
420 0.05) were implicated in sex determination, sex specific expression or gonad function in other
421 (fish) species (table S24) and ICS were significantly overrepresented among genes with
422 significant allele specific expression (Fisher's exact test $p = 1.6 \times 10^{-7}$). Furthermore, we found
423 candidate genes related to sex and reproduction among the strongest candidate genes for adaptive
424 evolution (i.e., those with the largest number nsICS) (Fig. 4D; text S3).

425 It is notable that for each of the three inversions with evidence for sex-linkage, the Y-like,
426 non-inverted haplotype arrived in the affected *benthics* through introgression events, affecting
427 mainly *eukambuzi*, other *shallow benthics/utaka*, and *deep benthics*, for chromosomes 9, 11, and
428 10, respectively (events ②, ③, and ④ in Fig. 3B). For chromosome 9, this is further supported-
429 by results from a lab based hybrid cross between females of *A. calliptera* and males of the
430 *eukambuzi* *Protomelas taeniolatus*, which showed a QTL peak for sex in the chromosome 9
431 inversion region (58). This is consistent with a dominant male-determining function of the
432 non-inverted *benthic* haplotype (with origin external to the Malawi radiation), even when paired
433 with an *A. calliptera* haplotype of the same orientation.

434 To further investigate the generality of the role of inversions in sex determination of
435 haplochromine cichlids, we applied our SNP-based inversion detection approach to publicly
436 available sequencing data for the Lake Victoria adaptive radiation (59). The results suggest that
437 the sex-linked regions identified by Feller et al. (58) on chromosomes 9 and 23 are in fact
438 chromosomal inversions (the one on chromosome 9 being distinct from the one present in
439 Malawi) (figs. S22 and S54), pointing to a wider relevance of chromosomal inversions in cichlid
440 sex determination.

441



442

443

444 **Fig. 5: Sex association of inversions.** (A) Windowed PC analysis along chromosome 11 demonstrates perfect
 445 association of inversion genotype with sex in our sample of 28 wild-caught *Copadichromis chrysonotus*. (B) SNP
 446 heterozygosity among our sample of wild-caught male and female *C. chrysonotus*, measured as number of het SNPs
 447 per 10 kbp. (C-E) Sex-inversion associations in lab-raised populations. Per population, the number of females and
 448 males is given (separated by '|') and asterisks denote significance levels of Fisher's exact tests of inversion
 449 genotype–sex correlation (*: p < 0.05, ***: p < 0.001). Inversion genotype per sex (confirmed through gonad
 450 examination) in lab-raised broods of (C) *C. chrysonotus* from Lake Malombe (p < 0.001, left) and from Lake Malawi
 451 (p = 0.048, right), (D) *Lethrinops chilingali* from satellite lake Chilingali (p < 0.001) (E), *Otopharynx tetrastigma* from
 452 Lake Malombe at the outflow of Lake Malawi (p < 0.001, left) and from the northern part of Lake Malawi (p = 0.049,
 453 right). (F) Proportions of homozygous/heterozygous inversion genotypes in males and females of species with
 454 heterozygotes present, according to WGS and PCR typing of 809 samples (67 species). Asterisks denote
 455 significance levels of Fisher's exact tests of inversion genotype–sex correlation (*: p < 0.05, ***: p < 0.001).

456 Discussion

457 In this article we identify large chromosomal inversions present in the Lake Malawi cichlid
458 radiation and present evidence that their evolutionary history was shaped by introgression,
459 ecological adaptation, and the turnover of sex determination systems. Our results are consistent
460 with a recent preprint that independently identified the inversions described here and their
461 sex-linkage based on optical mapping and chromosome-level de novo assemblies (60). Given the
462 evolutionarily independent presence of sex-linked inversions in Lake Victoria cichlids (fig. S54),
463 which are potentially also involved in adaptive introgression (59), and large scale differences in
464 male/female DNA sequence in Lake Tanganyika cichlids (61), we suggest that such
465 rearrangements may be a common feature of adaptive radiation in cichlids.

466 Chromosomal inversions have been implicated in adaptation, sex determination, and speciation
467 in many systems, especially in the context of adaptive divergence with gene flow (7, 11, 15–22,
468 28) likely because of their ability to lock together adaptive alleles (7). The chromosomal
469 inversions we identified in Malawi cichlids were involved in gene flow events at different stages
470 of the radiation, most prominently a founding admixture event of the species rich *benthic* clade
471 and introgression from a distantly related lineage outside the Malawi radiation (chromosome 9
472 inversion). These events coincide with bursts of eco-morphological diversification of the
473 resulting lineages. In the latter case, this concerns the *eukambuzi*, which show exceptional
474 diversity in eco-morphology, body patterning, and colouration (30).

475 We found evidence for inversion transmission between *deep* and *shallow benthic* species caught
476 at similar depths (fig. S35). At the same time, when not introgressed, inversions seemingly
477 helped to suppress gene flow and thereby contributed to adaptive divergence. However, despite
478 their excess divergence compared to the rest of the genome and the complete recombination
479 suppression we observed in a cross (Fig. 2E), most common genetic polymorphism is shared
480 across orientations suggesting that inversions are a barrier to genetic exchange rather than
481 completely suppressing it. On the one hand, this facilitates the purging of genetic load, which
482 often hinders the spread of inversions (62), while on the other hand, it provides an additional
483 mechanism for the creation of combinatorial diversity (5).

484 The genetic variants most differentiated between inverted and non-inverted haplotypes (ICS)
485 show a strong relative excess of amino acid changing mutations, as expected only under adaptive
486 evolution at many loci (text S3). These mutations showed enrichment in genes related to and
487 expressed in tissues involved in sensory and behavioural functions. This makes sense, because
488 sensory systems mediate sound perception, mechanoreception and vision, essential for
489 navigation and feeding in fishes (63), making them important targets of ecological adaptation to
490 differing underwater environments (64). Although further experiments – most promisingly
491 within species polymorphic for inversions – will be necessary to dissect the precise phenotypes

492 of the adaptive alleles within inversion regions, our results point towards widespread, multigenic
493 adaptation along a depth gradient which is a frequent axis of differentiation in fishes (65, 66).

494 We found evidence for XY-like sex linkage of the inversions on chromosomes 9, 10, and 11, in
495 which introgressed haplotypes of ancestral orientation act as Y chromosomes in some extant
496 species, with inversion-region genes related to sex and reproduction being under allele specific
497 expression in XY males and showing signatures of selection. Consistent with the highly dynamic
498 nature of sex determination in many fishes (67) and specifically cichlids (58, 61, 68), our results
499 point to a relatively easy recruitment of sex determination loci (SDLs), possibly as a direct
500 consequence of introgression of relatively divergent haplotypes affecting a sex determination
501 threshold, or due to heterozygote advantage of introgressed inversions selecting for the
502 recruitment of SDLs (69).

503 Sexual selection has been identified as a major predictor of successful radiation in cichlids (70),
504 and assortative mating is a main driver of cichlid reproductive isolation (71). Both of these
505 processes rely heavily on the same sensory systems (e.g., vision (71), olfaction (72), and hearing
506 (73)) that are also relevant for adaptation to depth and feeding niches, and that we identified as
507 candidates for adaptive evolution. Assortative mating and the evolution of sex linked regions are
508 both forms of sex-specific selection (74). Although the interplay between these forms of
509 selection is not well understood, it can give rise to synergistic evolutionary dynamics, potentially
510 mediated by sexually antagonistic selection (75, 76).

511 While our analysis focused on genetic variants nearly fixed between inversion haplotypes, we
512 expect that additional variants specific to particular species groups will prove important for
513 further diversification. Furthermore, alongside the inversions that identify admixture events, we
514 also see a signal of introgressed material in the rest of the genome, providing a potential
515 substrate for further selection and adaptation. Indeed, while we focussed on large inversions
516 segregating across many species, there are expected to be many more inversions and other
517 structural genetic variants that are smaller or have a more limited taxonomic distribution, as
518 suggested by our whole genome alignments and in Talbi et al. 2024 (77). Surely, more structural
519 variants with relevance in adaptive diversification are to be found in future studies.

520 In conclusion, the haplotypes of five chromosomal scale inversions in the Malawi cichlid
521 adaptive radiation show supergene-like signs of adaptive evolution and repeated introgression
522 associated with speciation. Together with the repeated transient sex-linked nature of introgressed
523 haplotypes, this provides a substrate for rich evolutionary dynamics around the interactions
524 between natural, sexual, and sexually antagonistic selection.

525 References and Notes

- 526 1. N. Eldredge, J. N. Thompson, P. M. Brakefield, S. Gavrilets, D. Jablonski, J. B. C. Jackson, R. E.
527 Lenski, B. S. Lieberman, M. A. McPeek, W. Miller, The dynamics of evolutionary stasis.
528 *Paleobiology* **31**, 133–145 (2005).
- 529 2. D. Berner, W. Salzburger, The genomics of organismal diversification illuminated by adaptive
530 radiations. *Trends Genet.* **31**, 491–499 (2015).
- 531 3. T. C. Nelson, W. A. Cresko, Ancient genomic variation underlies repeated ecological adaptation in
532 young stickleback populations. *Evolution Letters* **2**, 9–21 (2018).
- 533 4. J. I. Meier, D. A. Marques, S. Mwaiko, C. E. Wagner, L. Excoffier, O. Seehausen, Ancient
534 hybridization fuels rapid cichlid fish adaptive radiations. *Nat. Commun.* **8**, 14363 (2017).
- 535 5. D. A. Marques, J. I. Meier, O. Seehausen, A Combinatorial View on Speciation and Adaptive
536 Radiation. *Trends Ecol. Evol.* **34**, 531–544 (2019).
- 537 6. D. Roze, N. H. Barton, The Hill–Robertson Effect and the Evolution of Recombination. *Genetics*
538 **173**, 1793–1811 (2006).
- 539 7. M. Kirkpatrick, N. Barton, Chromosome inversions, local adaptation and speciation. *Genetics* **173**,
540 419–434 (2006).
- 541 8. A. Akerman, R. Bürger, The consequences of gene flow for local adaptation and differentiation: a
542 two-locus two-deme model. *J. Math. Biol.* **68**, 1135–1198 (2014).
- 543 9. R. K. Butlin, Recombination and speciation. *Mol. Ecol.* **14**, 2621–2635 (2005).
- 544 10. M. Kirkpatrick, How and why chromosome inversions evolve. *PLoS Biol.* **8** (2010).
- 545 11. M. Wellenreuther, L. Bernatchez, Eco-Evolutionary Genomics of Chromosomal Inversions. *Trends
546 Ecol. Evol.* **33**, 427–440 (2018).
- 547 12. M. Kirkpatrick, B. Barrett, Chromosome inversions, adaptive cassettes and the evolution of species’
548 ranges. *Mol. Ecol.* **24**, 2046–2055 (2015).
- 549 13. E. R. Hager, O. S. Harringmeyer, T. B. Wooldridge, S. Theingi, J. T. Gable, S. McFadden, B.
550 Neugeboren, K. M. Turner, J. D. Jensen, H. E. Hoekstra, A chromosomal inversion contributes to
551 divergence in multiple traits between deer mouse ecotypes. *Science* **377**, 399–405 (2022).
- 552 14. F. C. Jones, M. G. Grabherr, Y. F. Chan, P. Russell, E. Mauceli, J. Johnson, R. Swofford, M. Pirun,
553 M. C. Zody, S. White, E. Birney, S. Searle, J. Schmutz, J. Grimwood, M. C. Dickson, R. M. Myers,
554 C. T. Miller, B. R. Summers, A. K. Knecht, S. D. Brady, H. Zhang, A. A. Pollen, T. Howes, C.
555 Amemiya, Broad Institute Genome Sequencing Platform & Whole Genome Assembly Team, J.
556 Baldwin, T. Bloom, D. B. Jaffe, R. Nicol, J. Wilkinson, E. S. Lander, F. Di Palma, K. Lindblad-Toh,
557 D. M. Kingsley, The genomic basis of adaptive evolution in threespine sticklebacks. *Nature* **484**,
558 55–61 (2012).
- 559 15. R. Faria, A. Navarro, Chromosomal speciation revisited: rearranging theory with pieces of evidence.
560 *Trends Ecol. Evol.* **25**, 660–669 (2010).

561 16. D. Ayala, R. F. Guerrero, M. Kirkpatrick, Reproductive Isolation and Local Adaptation Quantified
562 for a Chromosome Inversion in a Malaria Mosquito. *Evolution* **67**, 946–958 (2013).

563 17. M. Joron, R. Papa, M. Beltrán, N. Chamberlain, J. Mavárez, S. Baxter, M. Abanto, E. Bermingham,
564 S. J. Humphray, J. Rogers, H. Beasley, K. Barlow, R. H. ffrench-Constant, J. Mallet, W. O.
565 McMillan, C. D. Jiggins, A conserved supergene locus controls colour pattern diversity in *Heliconius*
566 butterflies. *PLoS Biol.* **4**, e303 (2006).

567 18. K. Kunte, W. Zhang, A. Tenger-Trolander, D. H. Palmer, A. Martin, R. D. Reed, S. P. Mullen, M. R.
568 Kronforst, doublesex is a mimicry supergene. *Nature* **507**, 229–232 (2014).

569 19. C. Küpper, M. Stocks, J. E. Risso, N. Dos Remedios, L. L. Farrell, S. B. McRae, T. C. Morgan, N.
570 Karlionova, P. Pinchuk, Y. I. Verkuil, A. S. Kitaysky, J. C. Wingfield, T. Piersma, K. Zeng, J. Slate,
571 M. Blaxter, D. B. Lank, T. Burke, A supergene determines highly divergent male reproductive
572 morphs in the ruff. *Nat. Genet.* **48**, 79–83 (2016).

573 20. J. Wang, Y. Wurm, M. Nipitwattanaphon, O. Riba-Grognuz, Y.-C. Huang, D. Shoemaker, L. Keller,
574 A Y-like social chromosome causes alternative colony organization in fire ants. *Nature* **493**, 664–668
575 (2013).

576 21. P. R. Berg, B. Star, C. Pampoulie, M. Sodeland, J. M. I. Barth, H. Knutsen, K. S. Jakobsen, S.
577 Jentoft, Three chromosomal rearrangements promote genomic divergence between migratory and
578 stationary ecotypes of Atlantic cod. *Sci. Rep.* **6**, 23246 (2016).

579 22. M. A. F. Noor, K. L. Grams, L. A. Bertucci, J. Reiland, Chromosomal inversions and the
580 reproductive isolation of species. *Proceedings of the National Academy of Sciences* **98**, 12084–12088
581 (2001).

582 23. R. Castiglia, Sympatric sister species in rodents are more chromosomally differentiated than
583 allopatric ones: implications for the role of chromosomal rearrangements in speciation. *Mammal
584 Review* **44**, 1–4 (2014).

585 24. D. M. Hooper, T. D. Price, Chromosomal inversion differences correlate with range overlap in
586 passerine birds. *Nature Ecology & Evolution* **1**, 1526–1534 (2017).

587 25. C.-J. Rubin, E. D. Enbody, M. P. Dobreva, A. Abzhanov, B. W. Davis, S. Lamichhaney, M.
588 Pettersson, A. T. Sendell-Price, C. G. Sprehn, C. A. Valle, K. Vasco, O. Wallerman, B. R. Grant, P.
589 R. Grant, L. Andersson, Rapid adaptive radiation of Darwin's finches depends on ancestral genetic
590 modules. *Sci Adv* **8**, eabm5982 (2022).

591 26. D. Brawand, C. E. Wagner, Y. I. Li, M. Malinsky, I. Keller, S. Fan, O. Simakov, A. Y. Ng, Z. W. Lim,
592 E. Bezault, J. Turner-Maier, J. Johnson, R. Alcazar, H. J. Noh, P. Russell, B. Aken, J. Alföldi, C.
593 Amemiya, N. Azzouzi, J.-F. Baroiller, F. Barloy-Hubler, A. Berlin, R. Bloomquist, K. L. Carleton,
594 M. A. Conte, H. D'Cotta, O. Eshel, L. Gaffney, F. Galibert, H. F. Gante, S. Gnerre, L. Greuter, R.
595 Guyon, N. S. Haddad, W. Haerty, R. M. Harris, H. A. Hofmann, T. Hourlier, G. Hulata, D. B. Jaffe,
596 M. Lara, A. P. Lee, I. MacCallum, S. Mwaiko, M. Nikaido, H. Nishihara, C. Ozouf-Costaz, D. J.
597 Penman, D. Przybylski, M. Rakotomanga, S. C. P. Renn, F. J. Ribeiro, M. Ron, W. Salzburger, L.
598 Sanchez-Pulido, M. E. Santos, S. Searle, T. Sharpe, R. Swofford, F. J. Tan, L. Williams, S. Young, S.
599 Yin, N. Okada, T. D. Kocher, E. A. Miska, E. S. Lander, B. Venkatesh, R. D. Fernald, A. Meyer, C.
600 P. Ponting, J. T. Streelman, K. Lindblad-Toh, O. Seehausen, F. Di Palma, The genomic substrate for
601 adaptive radiation in African cichlid fish. *Nature* **513**, 375–381 (2014).

602 27. E. D. Enbody, A. T. Sendell-Price, C. G. Sprehn, C.-J. Rubin, P. M. Visscher, B. R. Grant, P. R.
603 Grant, L. Andersson, Community-wide genome sequencing reveals 30 years of Darwin's finch
604 evolution. *Science* **381**, eadf6218 (2023).

605 28. U. Krief, I. A. Müller, K. F. Stryjewski, D. Metzler, M. D. Sorenson, J. B. W. Wolf, Evolution of
606 Chromosomal Inversions across an Avian Radiation. *Mol Biol Evol* **41** (2024).

607 29. G. Barlow, *The Cichlid Fishes: Nature's Grand Experiment In Evolution* (Perseus Books Group,
608 2000).

609 30. A. Konings, *Malawi Cichlids in Their Natural Habitat* (Cichlid Press, 2016).

610 31. M. Malinsky, H. Svardal, A. M. Tyers, E. A. Miska, M. J. Genner, G. F. Turner, R. Durbin,
611 Whole-genome sequences of Malawi cichlids reveal multiple radiations interconnected by gene flow.
612 *Nat Ecol Evol*, doi: 10.1038/s41559-018-0717-x (2018).

613 32. H. Svardal, F. X. Quah, M. Malinsky, B. P. Ngatunga, E. A. Miska, W. Salzburger, M. J. Genner, G.
614 F. Turner, R. Durbin, Ancestral Hybridization Facilitated Species Diversification in the Lake Malawi
615 Cichlid Fish Adaptive Radiation. *Mol. Biol. Evol.* **37**, 1100–1113 (2020).

616 33. R. B. Stelkens, C. Schmid, O. Selz, O. Seehausen, Phenotypic novelty in experimental hybrids is
617 predicted by the genetic distance between species of cichlid fish. *BMC Evol. Biol.* **9**, 283 (2009).

618 34. R. A. York, C. Patil, K. Abdilleh, Z. V. Johnson, M. A. Conte, M. J. Genner, P. T. McGrath, H. B.
619 Fraser, R. D. Fernald, J. Todd Streelman, Behavior-dependent cis regulation reveals genes and
620 pathways associated with bower building in cichlid fishes. *Proceedings of the National Academy of
621 Sciences* **115**, E11081–E11090 (2018).

622 35. M. A. Conte, R. Joshi, E. C. Moore, S. P. Nandamuri, W. J. Gammerdinger, R. B. Roberts, K. L.
623 Carleton, S. Lien, T. D. Kocher, Chromosome-scale assemblies reveal the structural evolution of
624 African cichlid genomes. *Gigascience* **8** (2019).

625 36. O. S. Harringmeyer, H. E. Hoekstra, Chromosomal inversion polymorphisms shape the genomic
626 landscape of deer mice. *Nat Ecol Evol* **6**, 1965–1979 (2022).

627 37. P. Jay, M. Chouteau, A. Whibley, H. Bastide, H. Parrinello, V. Llaurens, M. Joron, Mutation load at a
628 mimicry supergene sheds new light on the evolution of inversion polymorphisms. *Nat. Genet.* **53**,
629 288–293 (2021).

630 38. A. Rhee, S. A. McCarthy, O. Fedrigo, J. Damas, G. Formenti, S. Koren, M. Uliano-Silva, W. Chow,
631 A. Fungtammasan, G. L. Gedman, L. J. Cantin, F. Thibaud-Nissen, L. Haggerty, C. Lee, B. J. Ko, J.
632 Kim, I. Bista, M. Smith, B. Haase, J. Mountcastle, S. Winkler, S. Paez, J. Howard, S. C. Vernes, T.
633 M. Lama, F. Grutzner, W. C. Warren, C. Balakrishnan, D. Burt, J. M. George, M. Biegler, D. Iorns,
634 A. Digby, D. Eason, T. Edwards, M. Wilkinson, G. Turner, A. Meyer, A. F. Kautt, P. Franchini, H.
635 William Detrich, H. Svardal, M. Wagner, G. J. P. Naylor, M. Pippel, M. Malinsky, M. Mooney, M.
636 Simbirsky, B. T. Hannigan, T. Pesout, M. Houck, A. Misuraca, S. B. Kingan, R. Hall, Z. Kronenberg,
637 J. Korlach, I. Sović, C. Dunn, Z. Ning, A. Hastie, J. Lee, S. Selvaraj, R. E. Green, N. H. Putnam, J.
638 Ghurye, E. Garrison, Y. Sims, J. Collins, S. Pelan, J. Torrance, A. Tracey, J. Wood, D. Guan, S. E.
639 London, D. F. Clayton, C. V. Mello, S. R. Friedrich, P. V. Lovell, E. Osipova, F. O. Al-Ajli, S.
640 Secomandi, H. Kim, C. Theofanopoulou, Y. Zhou, R. S. Harris, K. D. Makova, P. Medvedev, J.
641 Hoffman, P. Masterson, K. Clark, F. Martin, K. Howe, P. Flicek, B. P. Walenz, W. Kwak, H.

642 1. Clawson, M. Diekhans, L. Nassar, B. Paten, R. H. S. Kraus, H. Lewin, A. J. Crawford, M. T. P.
643 Gilbert, G. Zhang, B. Venkatesh, R. W. Murphy, K.-P. Koepfli, B. Shapiro, W. E. Johnson, F. Di
644 Palma, T. Margues-Bonet, E. C. Teeling, T. Warnow, J. M. Graves, O. A. Ryder, D. Hausler, S. J.
645 O'Brien, K. Howe, E. W. Myers, R. Durbin, A. M. Phillippy, E. D. Jarvis, Towards complete and
646 error-free genome assemblies of all vertebrate species, *Cold Spring Harbor Laboratory* (2020)p.
647 2020.05.22.110833.

648 39. H. Li, P. Ralph, Local PCA Shows How the Effect of Population Structure Differs Along the
649 Genome. *Genetics* **211**, 289–304 (2019).

650 40. L. S. Steviston, K. B. Hoehn, M. A. F. Noor, Effects of inversions on within- and between-species
651 recombination and divergence. *Genome Biol. Evol.* **3**, 830–841 (2011).

652 41. N. Patterson, P. Moorjani, Y. Luo, S. Mallick, N. Rohland, Y. Zhan, T. Genschoreck, T. Webster, D.
653 Reich, Ancient Admixture in Human History. *Genetics* **192**, 1065–1093 (2012).

654 42. N. Galtier, Half a Century of Controversy: The Neutralist/Selectionist Debate in Molecular
655 Evolution. *Genome Biol. Evol.* **16** (2024).

656 43. M. W. Hahn, *Molecular Population Genetics* (Sinauer Associates, Incorporated, 2018).

657 44. A. Sur, Y. Wang, P. Capar, G. Margolin, J. A. Farrell, Single-cell analysis of shared signatures and
658 transcriptional diversity during zebrafish development. *bioRxiv*, doi: 10.1101/2023.03.20.533545
659 (2023).

660 45. Z. Musilova, F. Cortesi, M. Matschiner, W. I. L. Davies, J. S. Patel, S. M. Stieb, F. de Busserolles, M.
661 Malmstrøm, O. K. Tørresen, C. J. Brown, J. K. Mountford, R. Hanel, D. L. Stenkamp, K. S.
662 Jakobsen, K. L. Carleton, S. Jentoft, J. Marshall, W. Salzburger, Vision using multiple distinct rod
663 opsins in deep-sea fishes. *Science* **364**, 588–592 (2019).

664 46. A. Brown, S. Thatje, Explaining bathymetric diversity patterns in marine benthic invertebrates and
665 demersal fishes: physiological contributions to adaptation of life at depth. *Biol. Rev. Camb. Philos.
666 Soc.* **89**, 406–426 (2014).

667 47. H.-S. Yim, Y. S. Cho, X. Guang, S. G. Kang, J.-Y. Jeong, S.-S. Cha, H.-M. Oh, J.-H. Lee, E. C.
668 Yang, K. K. Kwon, Y. J. Kim, T. W. Kim, W. Kim, J. H. Jeon, S.-J. Kim, D. H. Choi, S. Jho, H.-M.
669 Kim, J. Ko, H. Kim, Y.-A. Shin, H.-J. Jung, Y. Zheng, Z. Wang, Y. Chen, M. Chen, A. Jiang, E. Li,
670 S. Zhang, H. Hou, T. H. Kim, L. Yu, S. Liu, K. Ahn, J. Cooper, S.-G. Park, C. P. Hong, W. Jin, H.-S.
671 Kim, C. Park, K. Lee, S. Chun, P. A. Morin, S. J. O'Brien, H. Lee, J. Kimura, D. Y. Moon, A.
672 Manica, J. Edwards, B. C. Kim, S. Kim, J. Wang, J. Bhak, H. S. Lee, J.-H. Lee, Minke whale
673 genome and aquatic adaptation in cetaceans. *Nat. Genet.* **46**, 88–92 (2014).

674 48. M. Malinsky, R. J. Challis, A. M. Tyers, S. Schiffels, Y. Terai, B. P. Ngatunga, E. A. Miska, R.
675 Durbin, M. J. Genner, G. F. Turner, Genomic islands of speciation separate cichlid ecomorphs in an
676 East African crater lake. *Science* **350**, 1493–1498 (2015).

677 49. C. Hahn, M. J. Genner, G. F. Turner, D. A. Joyce, The genomic basis of cichlid fish adaptation
678 within the deepwater “twilight zone” of Lake Malawi. *Evol Lett* **1**, 184–198 (2017).

679 50. S. L. Mederos, R. C. Duarte, M. Mastoras, M. Y. Dennis, M. L. Settles, A. R. Lau, A. Scott, K.
680 Woodward, C. Johnson, A. M. H. Seelke, K. L. Bales, Effects of pairing on color change and central

681 gene expression in lined seahorses. *Genes Brain Behav.* **21**, e12812 (2022).

682 51. Z. V. Johnson, B. E. Hegarty, G. W. Gruenhagen, T. J. Lancaster, P. T. McGrath, J. T. Streelman,
683 Cellular profiling of a recently-evolved social behavior in cichlid fishes. *Nat. Commun.* **14**, 4891
684 (2023).

685 52. I. S. Magalhaes, A. M. Smith, D. A. Joyce, Quantifying mating success of territorial males and
686 sneakers in a bower-building cichlid fish. *Sci. Rep.* **7**, 41128 (2017).

687 53. D. Bachtrog, Y-chromosome evolution: emerging insights into processes of Y-chromosome
688 degeneration. *Nat. Rev. Genet.* **14**, 113–124 (2013).

689 54. C. L. Peichel, S. R. McCann, J. A. Ross, A. F. S. Naftaly, J. R. Urton, J. N. Cech, J. Grimwood, J.
690 Schmutz, R. M. Myers, D. M. Kingsley, M. A. White, Assembly of the threespine stickleback Y
691 chromosome reveals convergent signatures of sex chromosome evolution. *Genome Biol.* **21**, 177
692 (2020).

693 55. J. R. Ser, R. B. Roberts, T. D. Kocher, Multiple interacting loci control sex determination in lake
694 Malawi cichlid fish. *Evolution* **64**, 486–501 (2010).

695 56. H. Munby, T. Linderoth, B. Fischer, M. Du, G. Vernaz, A. M. Tyers, B. P. Ngatunga, A. Shechonge,
696 H. Denise, S. A. McCarthy, I. Bista, E. A. Miska, M. E. Santos, M. J. Genner, G. F. Turner, R.
697 Durbin, Differential use of multiple genetic sex determination systems in divergent ecomorphs of an
698 African crater lake cichlid (2021). <https://doi.org/10.1101/2021.08.05.455235>.

699 57. Q. Zhou, D. Bachtrog, Chromosome-wide gene silencing initiates Y degeneration in *Drosophila*.
700 *Curr. Biol.* **22**, 522–525 (2012).

701 58. A. F. Feller, V. Ogi, O. Seehausen, J. I. Meier, Identification of a novel sex determining chromosome
702 in cichlid fishes that acts as XY or ZW in different lineages. *Hydrobiologia* **848**, 3727–3745 (2021).

703 59. M. D. McGee, S. R. Borstein, J. I. Meier, D. A. Marques, S. Mwaiko, A. Taabu, M. A. Kishe, B.
704 O’Meara, R. Bruggmann, L. Excoffier, O. Seehausen, The ecological and genomic basis of explosive
705 adaptive radiation. *Nature* **586**, 75–79 (2020).

706 60. N. M. Kumar, T. L. Cooper, T. D. Kocher, J. T. Streelman, P. T. McGrath, Large inversions in Lake
707 Malawi cichlids are associated with habitat preference, lineage, and sex determination. eLife
708 Sciences Publications, Ltd [Preprint] (2025). <https://doi.org/10.7554/elife.104923.1>.

709 61. A. El Taher, F. Ronco, M. Matschiner, W. Salzburger, A. Böhne, Dynamics of sex chromosome
710 evolution in a rapid radiation of cichlid fishes. *Sci Adv* **7**, eabe8215 (2021).

711 62. E. L. Berdan, A. Blanckaert, R. K. Butlin, C. Bank, Deleterious mutation accumulation and the
712 long-term fate of chromosomal inversions. *PLoS Genet* **17**, e1009411 (2021).

713 63. D. Escobar-Camacho, K. L. Carleton, Sensory modalities in cichlid fish behavior. *Curr Opin Behav*
714 *Sci* **6**, 115–124 (2015).

715 64. Z. Musilova, W. Salzburger, F. Cortesi, The Visual Opsin Gene Repertoires of Teleost Fishes:
716 Evolution, Ecology, and Function. *Annu. Rev. Cell Dev. Biol.* **37**, 441–468 (2021).

717 65. M. Barluenga, K. N. Stölting, W. Salzburger, M. Muschick, A. Meyer, Sympatric speciation in
718 Nicaraguan crater lake cichlid fish. *Nature* **439**, 719–723 (2006).

719 66. M. Malinsky, R. J. Challis, A. M. Tyers, S. Schiffels, Y. Terai, B. P. Ngatunga, E. A. Miska, R.
720 Durbin, M. J. Genner, G. F. Turner, Genomic islands of speciation separate cichlid ecomorphs in an
721 East African crater lake. *Science* **350**, 1493–1498 (2015).

722 67. J. Kitano, S. Ansai, S. Fujimoto, R. Kakioka, M. Sato, I. F. Mandagi, B. K. A. Sumarto, K.
723 Yamahira, A Cryptic Sex-Linked Locus Revealed by the Elimination of a Master Sex-Determining
724 Locus in Medaka Fish. *Am. Nat.* **202**, 231–240 (2023).

725 68. W. J. Gammerdinger, T. D. Kocher, Unusual Diversity of Sex Chromosomes in African Cichlid
726 Fishes. *Genes* **9** (2018).

727 69. P. Jay, E. Tezenas, A. Véber, T. Giraud, Sheltering of deleterious mutations explains the stepwise
728 extension of recombination suppression on sex chromosomes and other supergenes. *PLoS Biol.* **20**,
729 e3001698 (2022).

730 70. C. E. Wagner, L. J. Harmon, O. Seehausen, Ecological opportunity and sexual selection together
731 predict adaptive radiation. *Nature* **487**, 366–369 (2012).

732 71. O. M. Selz, M. E. R. Pierotti, M. E. Maan, C. Schmid, O. Seehausen, Female preference for male
733 color is necessary and sufficient for assortative mating in 2 cichlid sister species. *Behav. Ecol.* **25**,
734 612–626 (2014).

735 72. M. Plenderleith, C. van Oosterhout, R. L. Robinson, G. F. Turner, Female preference for conspecific
736 males based on olfactory cues in a Lake Malawi cichlid fish. *Biol. Lett.* **1**, 411–414 (2005).

737 73. K. P. Maruska, U. S. Ung, R. D. Fernald, The African cichlid fish *Astatotilapia burtoni* uses acoustic
738 communication for reproduction: sound production, hearing, and behavioral significance. *PLoS One*
739 **7**, e37612 (2012).

740 74. A. E. Wright, J. E. Mank, The scope and strength of sex-specific selection in genome evolution. *J.
741 Evol. Biol.* **26**, 1841–1853 (2013).

742 75. P. Muralidhar, Mating preferences of selfish sex chromosomes. *Nature* **570**, 376–379 (2019).

743 76. S. H. Smith, K. Hsiung, A. Böhne, Evaluating the role of sexual antagonism in the evolution of sex
744 chromosomes: new data from fish. *Curr. Opin. Genet. Dev.* **81**, 102078 (2023).

745 77. M. Talbi, G. F. Turner, M. Malinsky, Rapid evolution of recombination landscapes during the
746 divergence of cichlid ecotypes in Lake Masoko, *bioRxiv* (2024).
747 <https://doi.org/10.1101/2024.03.20.585960>.

748

749 Acknowledgments

750 We thank the Department of Fisheries of the Government of Malawi for facilitating Malawi
751 cichlid specimen collection and Martin Genner, Alix Tyers, Mingliu Du, Mexford Mulumpwa,
752 Magnus Nordborg, Karl Svardal and the staff of the Monkey Bay Fisheries Research Unit for
753 support with sampling, Shane McCarthy for bioinformatics support, Walter Salzburger for access
754 to facilities and data, and Patrick Gemmell for input on the project. We are grateful to Daniel
755 Shaw, Regev Schweiger, Victoria Caudill, Peter Ralph, Jonas Lescroart, and Els De Keyzer for
756 useful comments on the manuscript.

757

758 Funding

759 The authors gratefully acknowledge support through the Research Foundation – Flanders (FWO)
760 (G047521N to H.S.), the Wellcome Trust (Wellcome grant 207492 to R.D., Wellcome Senior
761 Investigator Award 219475/Z/19/Z to E.A.M), the Research Fund of the University of Antwerp
762 (BOF) (to H.S.), the Cambridge-Africa ALBORADA Research Fund (to H.S. and B.R.), the
763 German Research Foundation (DFG) (492407022 and 497674620 to A.B.), the European
764 Research Council (Proof-of-Concept Grant 101069219 to M.K. and Y.F.C.), the Max Planck
765 Society (to Y.F.C.), and the Natural Environment Research Council (NERC) (IRF
766 NE/R01504X/1 to M.E.S.). L.M.B. was supported through a Harding Distinguished Postgraduate
767 Scholarship and S.G. through an FWO PhD Fellowship Fundamental Research. G.V.
768 acknowledges Wolfson College University of Cambridge and the Genetics Society London for
769 financial support.

770 Authors contributions

771 H.S. and R.D. conceived the study, with support from L.M.B. H.S. organised cichlid collections
772 in Malawi with support from B.R., R.Z., W.S., J.C.G, M.N., M.M., R.D., G.V., E.A.M., and
773 G.F.T. G.F.T. undertook final taxonomic assignment. I.B. and V.B. performed DNA extractions.
774 T.L. produced the original variant callset. H.S., L.M.B., V.B., I.A., J.S., and J.C.G. analysed the
775 SNP data. Inversion detection was accomplished by L.M.B. (PCA-based) and I.A.
776 (clusterization, phylogenetic reconstructions). H.S. performed hybridisation analysis. V.B. made
777 selection tests (together with H.S.), zebrafish-based functional analysis and candidate genes
778 investigation. J.C.G. performed enrichment analysis and candidate gene investigation. J.S. and
779 H.S. performed population history reconstructions. J.E., A.H., M.E.S., and G.F.T. performed the
780 species cross. B.F. designed the PCR essays and provided molecular lab support. V.B. performed
781 PCR typing. C.Z., L.M.B. and B.F. produced assemblies and analysed long read and Hi-C data
782 with support from J.S. F.C.J. performed and analysed time-foward simulations. A.H.H. raised
783 and collected lab populations for sex determination analysis. N.H. performed PCR-typing of lab
784 populations. L.M.B. detected sex-linked inversions in the Lake Victoria radiation. M.K. and
785 Y.F.C. performed haplotagging. I.A. analysed haplotagging data. W.S., I.A., and H.S. analysed

786 RNA-seq data. S.L. and F.Y. performed FISH. S.G. produced and analysed the outgroup variant
787 callset with support from H.S. M.M. produced Hi-C data and the ancestral sequence. D.A.J.
788 contributed the *Diplotaxodon* long read samples. A.B. provided support for sex chromosome and
789 adaptation related analyses. L.M.B. designed the main figures, with input from H.S., V.B., J.C.
790 and I.A. H.S. wrote the initial manuscript. H.S., R.D., L.M.B., V.B., and J.C. edited the
791 manuscript with contributions from all authors. All authors read and approved the final
792 manuscript.

793 Competing interests

794 The authors declare that there are no competing interests.

795 Data and materials availability

796 Supporting data is made available in the online supplementary on an open-access basis for
797 research use only. ENA Accession numbers of raw sequencing data <will be added to
798 Supplementary Table 1 before final publication>. VCF are shared in Dryad repository <DOI
799 added before final publication>. Data was collected under appropriate ethical and sampling
800 permits and genetic material and sequences are subject to an Access and Benefits Sharing (ABS)
801 agreement with the Government of Malawi. Any person who wishes to use this data for any form
802 of commercial purpose must first enter into a commercial licensing and benefit-sharing
803 arrangement with the Government of Malawi.

804

805 Supplementary Materials

806 Materials and Methods

807 Supplementary Text

808 Fig. S1 to Fig. S54

809 Table S1 to S31

810 References (78-177)

811 Data S1 to S8